

Self-Diffusion of Hydrophilic Poly(propyleneimine) Dendrimers in Poly(vinyl alcohol) Solutions and Gels by Pulsed Field Gradient NMR Spectroscopy

W. E. Baille, C. Malveau, and X. X. Zhu*

Département de Chimie, Université de Montréal, C.P. 6128, Succ. Centre-ville, Montréal, Québec, Canada H3C 3J7

Y. H. Kim and W. T. Ford

Department of Chemistry, Oklahoma State University, Stillwater, Oklahoma 74078

Received August 30, 2002; Revised Manuscript Received November 25, 2002

ABSTRACT: Pulsed-field gradient NMR spectroscopy was used to study the diffusion of three different poly(propyleneimine) dendrimers with hydrophilic triethylenoxy methyl ether terminal groups (generations 2, 4, and 5) in poly(vinyl alcohol) aqueous solutions and gels. The effects of the diffusant size, polymer concentration (from 0 to 0.26 g/mL), and temperature on the self-diffusion coefficients have been studied, and the model of Petit et al. [*Macromolecules* 1996, 29, 6031] was used to fit the experimental data. The Stokes–Einstein hard-sphere radii were also calculated in the zero concentration limit and were compared with those of the linear poly(ethylene glycol)s under the same conditions. The proton NMR relaxation times (T_1 and T_2) were measured to study the mobility of the dendrimer core part and terminal group as a function of the dendrimer size.

Introduction

The diffusion of various solute molecules in polymer solutions and gels is very important in the application of polymer solutions and gels. Examples include permeation through polymer membranes,¹ diffusion of plasticizers in plastic materials,² and drug release from polymer gels.³ The study of self-diffusion of different solutes and additives in polymers may help in the elucidation of the effects of polymer concentration, size and shape of the diffusant, temperature, and specific interactions within the polymer network.⁴ The information is critical in determining the applicability of polymeric materials in industry. Various physical models of diffusion have been proposed over the years.^{5–13} These physical models of diffusion are essential for the interpretation of the results. Pulsed-field gradient (PFG) NMR techniques have been used successfully in the study of self-diffusion of solute and solvent molecules in polymer solutions and gels.^{4,11,14–24}

We have previously studied the self-diffusion in polymer solutions and gels of solute molecules ranging from small molecules to polymers.^{4,11,25–28} The results obtained by the study of the diffusion of small diffusants with different functional groups (alcohol, amine, ammonium salt, amide, and acid) in poly(vinyl alcohol) (PVA) solutions and gels show that the diffusion behavior is primarily influenced by the size of the diffusant and secondarily by the chemical interactions.²⁵ For the self-diffusion of linear oligo- and poly(ethylene glycol)s (PEGs) the molecular size of the diffusant plays the most important part in the diffusion process.^{4,25,27} The effect of the polymer matrices on the self-diffusion of PEG with molecular weight 600 was also studied for different ternary polymer–water–PEG systems.²⁶ The diffusion of the PEG did not vary significantly with the

molecular weight of the PVA matrix, and only a small variation was observed with the degree of hydrolysis of the PVA. The diffusion in hydrophilic polymers is mostly affected by formation of the hydrogen bonds between the solute and the polymer matrix. All these studies have allowed us to test the applicability of a new physical model developed by our group.¹¹ This model have been used successfully to describe the effect of the polymer concentration, the temperature, and the diffusant size on the diffusion process in polymer gels.

The PEG diffusants used in our studies so far differed in their molecular weights^{4,27} and sometimes in their chain-end groups,²⁸ but they are all linear polymers. A hydrodynamic radius can be estimated for such molecules in solution, but the exact process of diffusion of these linear oligomers and polymers in a gel matrix remains to be clarified. In addition, there is a problem of polydispersity of the PEG samples even after fractionation. It would be interesting to compare their behavior with that of more spherical molecules with similar molecular weights but different sizes of the cross sections. Dendritic polymers are molecules of choice because of the good control in their molecular size and shape (more spherical). Moreover, dendritic polymers have a more regular conformation and a lower degree of polydispersity in comparison to highly branched polymers.^{29–32} These characteristics make dendrimers very interesting and useful as a model diffusion probes. Also, they can be used in many different applications such as molecular encapsulation for drug delivery, membrane transport, or molecular recognition.^{33,34} Therefore, the self-diffusion process of three different poly(propyleneimine) (PPI) dendrimers with hydrophilic triethylenoxy methyl ether (TEO) terminal groups in PVA aqueous solutions and gels was studied by the PFG NMR technique. The effects of polymer concentration, temperature, and dendrimer size on the self-diffusion coefficients were investigated. We have also studied the

* To whom correspondence should be addressed. E-mail: julian.zhu@umontreal.ca.

mobility of the dendrimer core part and terminal group as a function of generation by the measurement of ^1H NMR relaxation times (T_1 and T_2).

Experimental Section

Materials. DAB-*dendr*-(NH_2) $_n$ ($n = 8, 32,$ and 64) and all other chemicals were purchased from Aldrich (Milwaukee, WI). Triethylamine (TEA) was dried over anhydrous 3 \AA molecular sieves and freshly distilled. All other chemicals were used as received. D_2O was purchased from C.I.L. (Andover, MA).

2-[2-(2-Methoxyethoxy)ethoxy]acetyl Chloride. A solution of 2-[2-(2-methoxyethoxy)ethoxy]acetic acid (5.34 g, 30.0 mmol) and oxalyl chloride (6.35 g, 50.0 mmol) in 3 mL of toluene was stirred for 4 h at $65 \text{ }^\circ\text{C}$. The solvent and excess reagent were removed under reduced pressure, and the residue was dried at $40 \text{ }^\circ\text{C}$ under vacuum to give a light yellow oil (5.34 g, 90%) which was used without further purification.

Modified Poly(propyleneimine) Dendrimers.^{35,36} 2-[2-(2-Methoxyethoxy)ethoxy]acetyl chloride (3.00 g, 15.3 mmol) was added to a solution of PPI dendrimer DAB-*dendr*-(NH_2) $_8$ (1.00 g, 1.29 mmol), DMF (5.0 mL), and TEA (0.9 g, 8.89 mmol) at $0 \text{ }^\circ\text{C}$. The solution was stirred under nitrogen at $70 \text{ }^\circ\text{C}$ for 24 h. Water (5 mL) was added to hydrolyze the excess acid chloride. The mixture was made basic to $\text{pH} > 14$ using 5 g (27 mmol) of tetramethylammonium hydroxide pentahydrate and was extracted with CH_2Cl_2 (4 times 10 mL). The combined dichloromethane solution was dried over Na_2SO_4 and evaporated. The oily residue was dried at $40 \text{ }^\circ\text{C}$ under vacuum to give a light yellow oil of PPI(TEO) $_8$ (2.21 g, 83%). DAB-*dendr*-(NH_2) $_n$ ($n = 32$ and 64) were also modified with triethylenoxy methyl ether end groups by the same procedure to yield PPI(TEO) $_{32}$ and PPI(TEO) $_{64}$. The ^1H and ^{13}C NMR spectra of dendrimers made by a slightly different procedure were the same as the spectra of those reported here.^{35,36}

Sample Preparation. Samples were prepared following the method described previously.^{4,11} PVA ($M_n = 52\,000$ with a degree of hydrolysis = 99%) was added to a D_2O solution containing 1 wt % of dendrimer probes in 5 mm o.d. NMR tubes. The NMR tubes were sealed to avoid solvent evaporation and heated at temperature between 100 and $110 \text{ }^\circ\text{C}$ to dissolve the PVA and to help in the mixing of the sample. The heating helped also to prevent gelation effects. The concentration of PVA ranged from 0 to 0.26 g/mL.

Molecular Weight Determination. ^1H NMR experiments were performed on a Bruker AMX-300 spectrometer operating at a frequency of 300.13 MHz to determine the molecular weights (M_n) of the dendrimer, based on the ratio of the integrated peak areas of the methylene protons at 4.05 ppm to the methylene groups in the core.

Relaxation Time Measurements. ^1H spin-lattice (T_1) and spin-spin (T_2) relaxation times were measured on a Bruker AMX-300 spectrometer operating at 300.13 MHz. Experiments were conducted at $25 \text{ }^\circ\text{C}$. T_1 was obtained with the classical inversion-recovery pulse sequences. All measurements were performed using eight scans with a repetition time of 30 s. A total of 24 increments of the recovery time between 0.01 and 25 s were used. The T_1 values were extracted by the use of

$$\frac{M}{M_0} = \left[1 - k \exp\left(-\frac{\tau}{T_1}\right) \right] \quad (1)$$

where M_0 and M are the magnetization at equilibrium and for a recovery time τ , respectively; T_1 and k can be calculated by least mean square method. The variable k is ideally equal to 2, but for all experiments k obtained are between 1.8 and 2.0. T_2 measurements were performed with the classical Carr-Purcell-Meiboom-Gill (CPMG) pulse sequences. The T_2 values were extracted from

$$\frac{M}{M_0} = \exp\left(-\frac{2\tau n}{T_2}\right) \quad (2)$$

where M_0 and M are the magnetization at the equilibrium and at the n th echo, respectively. τ is a fixed echo time (set at 2 ms), which allows the attenuation of diffusion and J -modulation effects, and n is an even number of echoes (32 values between 2 and 2400 echoes were chosen).

Pulsed Field Gradient NMR Measurements. The self-diffusion coefficient (D) measurements were performed using the stimulated echo (STE: $90^\circ-t_1-90^\circ-t_2-90^\circ-t_1$ -echo) sequence developed by Tanner³⁷ on a Bruker DSX-300 NMR spectrometer operating at a frequency of 300.18 MHz for protons. A Bruker imaging probe (Micro2.5 probe) was used with a three orthogonal field gradient coils system permitting a maximum gradient of 100 G/cm. The self-diffusion coefficients were obtained from the attenuation of the NMR signals due to the application of the gradient pulses of various strengths in a stimulated echo sequence, as given in the following expression³⁸⁻⁴⁰

$$\ln \frac{I}{I_0} = -\frac{t_2}{T_1} - \frac{2t_1}{T_2} - \ln 2 - \gamma^2 \delta^2 G^2 D (\Delta - \delta/3) \quad (3)$$

where I and I_0 are the NMR signal intensities in the presence and in the absence of the gradient, respectively, t_1 is the interval between the first two 90° rf pulses and between the third 90° rf pulse and the middle of the echo, t_2 is the delay between the second and the third 90° rf pulses, γ is the gyromagnetic ratio of the nucleus under observation, δ and G are the duration and the strength of the applied gradient pulse, respectively, D is the self-diffusion coefficient, and Δ is the time interval between the two successive gradient pulses (also called the diffusion time). The self-diffusion coefficient was extracted from the slopes of the lines obtained from linear regression of the logarithm of signal intensity as a function of G^2 . Excellent linear relationships have been obtained in these experiments with correlation coefficients of 0.996 and better. The error of the measured D values was estimated to be $\leq 5\%$ by carrying out repeated experiments with selected samples.

The experiments were performed at different temperatures from 5 to $45 \text{ }^\circ\text{C}$ (fluctuation of the temperature $\pm 0.3 \text{ }^\circ\text{C}$), and concentrations of PVA ranged from 0 to 0.26 g/mL. Temperature calibration was done periodically on the NMR instrument by measuring the chemical shift difference between the ^1H NMR signals of CH_2 and OH groups of pure ethylene glycol at various temperatures since this difference is sensitive to temperature changes.⁴¹

A nonlinear least-squares fitting method was used in all cases to fit the experimental diffusion data to the model of Petit et al.¹¹ The correlation coefficients r^2 yielded were in the range 0.997–0.999. The quality of the fitting to the experimental data was also indicated by the good fits shown in all the figures. The same sets of fitting parameters were obtained regardless of the initial values used in the procedure.

Results and Discussion

NMR Characterization. ^1H NMR spectra of the synthesized products were done in D_2O at 1 wt % of the dendrimers. The reaction of the amine groups on the dendrimer surface with TEO is evidenced by the high field shift of the methylene protons from 4.75 ppm (for TEO before reaction) to 4.05 ppm (peak labeled f in Figure 1). These spectra also confirm the structure of dendrimers. All the proton signals of the dendrimers are assigned (Figure 1). The NMR spectra were also used to determine the molecular weight of these dendrimers (Table 1). The molecular weight was obtained from the integrated area ratio of methylene protons at 4.05 ppm (peak f) and methylene protons at 1.73 ppm. The comparison between the values expected for an ideal dendrimer growth and the values determined experimentally by ^1H NMR spectroscopy allows the determination of the molecular weight. This ratio also helps to determine the completeness of the end groups

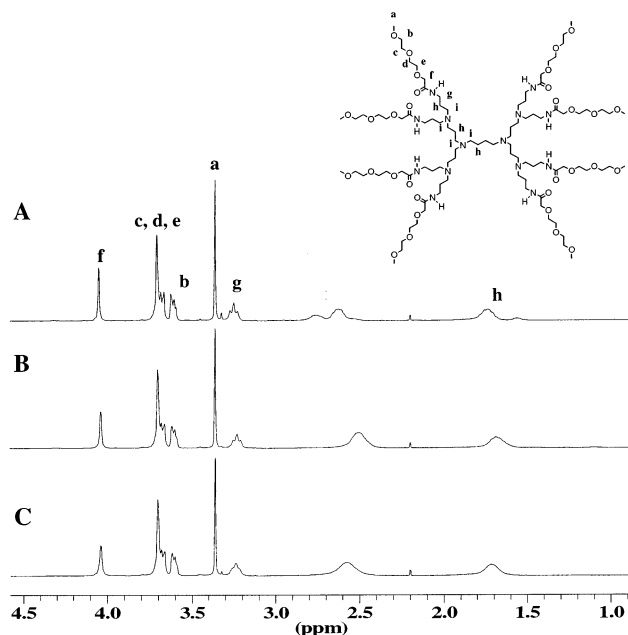


Figure 1. ^1H NMR spectra of three different poly(propyleneimine) dendrimers with hydrophilic triethylenoxy methyl ether terminal groups at 1 wt % in D_2O at 25°C : (A) PPI(TEO) $_8$, (B) PPI(TEO) $_{32}$, (C) PPI(TEO) $_{64}$.

Table 1. Some Characteristics of the Modified Poly(propyleneimine) Dendrimers

samples	no. of generations	terminal groups	M^a (g/mol)	M_n^b (g/mol)
PPI(TEO) $_8$	2	8	2055	2000
PPI(TEO) $_{32}$	4	32	8639	8600
PPI(TEO) $_{64}$	5	64	17396	17000

^a Molecular weight calculated for ideal dendrimer growth.

^b Number-average molecular weight determined by ^1H NMR spectroscopy.

Table 2. NMR Relaxation Times for the Different ^1H Signals of the Dendrimers at 25°C

sample	NMR peaks ^a				
	a	b	f	h	i
spin-spin relaxation times, T_1 (s)					
PPI(TEO) $_8$	2.48	0.64	0.50	0.24	0.21
PPI(TEO) $_{32}$	1.88	0.52	0.46	0.28	0.28
PPI(TEO) $_{64}$	1.64	0.49	0.45	0.31	0.31
spin-lattice relaxation times, T_2 (s)					
PPI(TEO) $_8$	2.02	0.42	0.26	0.04	0.04
PPI(TEO) $_{32}$	1.21	0.29	0.16	0.03	0.03
PPI(TEO) $_{64}$	0.94	0.22	0.11	0.02	0.02

^a Peaks a, b, f, h, and i correspond to the proton signals as identified in Figure 1.

amidation. The experimental intensity ratio obtained for each dendrimer generation shows that the modified poly(propyleneimine) dendrimers synthesized are practically ideal.

Relaxation Times Measurements. ^1H NMR relaxation times (T_1 and T_2) were measured to study the motions of three different parts of the dendrimers (methyl and methylene protons of the terminal groups and methylene protons of the core) as a function of generation. The results obtained are listed in Table 2. All dendrimers showed a sharp decrease (ca. 50 times) in the T_2 from the methyl protons of the terminal groups (peak a) to the methylene protons of the core (peaks h and i). Moreover, a large difference is observed among

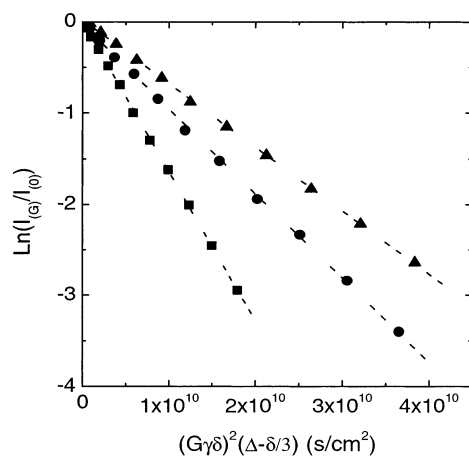


Figure 2. Semilogarithmic plot of the attenuation of the dendrimer NMR signals in a 1 wt % aqueous solution (without PVA) at 25°C as a function of $(G\gamma\delta)^2(\Delta - \delta/3)$. $\delta = 1.0$ ms, $\Delta = 400$ ms. Squares, PPI(TEO) $_8$; circles, PPI(TEO) $_{32}$; and triangles, PPI(TEO) $_{64}$.

the three distinct zones. This result indicates that the mobility increases from the inner core of the dendrimers to the outer part. Table 2 also shows a decrease in T_2 at higher generations of the dendrimers. A decrease by a factor of ca. 2 was observed between the PPI(TEO) $_8$ and the PPI(TEO) $_{64}$ for all peaks, indicating a decrease in the mobility of the dendrimers. In the measurements of ^1H T_1 , for the terminal groups a decrease in the T_1 was observed with increasing dendrimer generation, but an increase in the T_1 was observed for core protons. This may be related to the relative mobility of the different parts of the dendrimers. The terminal protons are more mobile and still lie in the extreme narrowing region, corresponding to short correlation times, while the protons in the core of the dendrimers are less mobile and correspond to longer correlation times lying on the right side of the T_1 minimum on the curve of T_1 as a function of the correlation time. Therefore, there is no contradiction with the T_2 results since T_2 generally decreases as a function of molecular correlation time.

Diffusion Measurements. Figure 2 is a semilogarithmic plot of the attenuation of the NMR signals as a function of $\gamma^2\delta^2G^2(\Delta - \delta/3)$ with δ and Δ equal to 1.0 and 400 ms, respectively. According to eq 3, this relationship is linear if the diffusion is isotropic and the slope of the line equals $-D$. All self-diffusion coefficient measurements presented in this paper were performed on the methyl protons labeled a (see Figure 1). However, we have verified that the self-diffusion coefficient is the same for all protons. Moreover, the self-diffusion coefficient was determined on all directions (x , y , and z) of the applied gradient pulse to verify whether the diffusion is isotropic. The results obtained show that D is independent of the direction. Attempts were made to detect restricted diffusion of the dendrimers by measuring their self-diffusion coefficient as a function of diffusion time Δ from 20 to 600 ms for the dendrimers with two different PVA concentrations (0.12 and 0.26 g/mL). At each of the PVA concentrations, the self-diffusion coefficients obtained as a function of diffusion time are identical, indicating that no restricted diffusion is present. The excellent linearity observed in Figure 2 indicates that the self-diffusion coefficients are monodisperse, and the D values obtained decrease with the increase in the generation or hence the molecular weight of the dendrimers. The decrease in D values can be

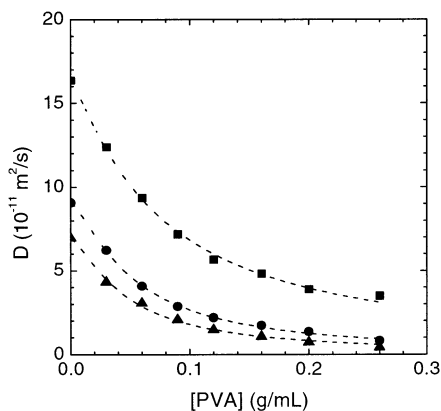


Figure 3. Dendrimers self-diffusion coefficients as a function of PVA concentration at 25 °C. Dashed lines are fits to eq 7. Squares, PPI(TEO)₈; circles, PPI(TEO)₃₂; and triangles, PPI(TEO)₆₄.

described by the following expression in the case of an uncharged spherical particle at infinite dilution moving in laminar flow:⁴²

$$D = \frac{RT}{2^{1/3} 3^{4/3} \pi^{4/3} N^{2/3} \bar{v}^{1/3} M^{1/3} \eta} \quad (4)$$

where D is the self-diffusion coefficient, R is the gas constant, T is the absolute temperature, η is the viscosity of the solvent (D_2O), N is the Avogadro's number, \bar{v} is the experimentally determinable partial specific volume of the diffusing molecule, and M is the molecular weight of the diffusant. Equation 4 is obtained from the Stokes–Einstein equation

$$D_0 = \frac{k_B T}{6\pi\eta R_h} \quad (5)$$

where D_0 is the self-diffusion coefficient at zero polymer concentration, k_B is the Boltzmann constant, and R_h is the effective hydrodynamic radius of the diffusing molecule, which is related to \bar{v} and M by the following expression:⁴²

$$R_h = \sqrt[3]{\frac{3M\bar{v}}{4\pi N}} \quad (6)$$

By substituting eq 6 into eq 5, the relationship between the diffusion coefficient and the molecular weight (eq 4) can be obtained. From eq 4 and without any specific interaction process between the diffusant and the polymer, the self-diffusion coefficient is inversely proportional to the cubic root of the molecular weight, which explains the decrease of D with the increase of dendrimer size.

(1) Effect of Polymer Concentration. The self-diffusion coefficients of these dendrimers as a function of PVA concentration are shown in Figure 3. This figure shows a decrease in the D values with the PVA concentration, from 0 to 0.26 g/mL. The concentration range includes the dilute and the viscous gel regimes. The decrease of the self-diffusion coefficient with PVA concentration can be described by the correlation length ξ , which represents the mesh size of a transient statistical network. As illustrated by de Gennes's scaling theory⁴³ ($\xi = \beta c^{-\nu}$, where β should be a constant and does not vary as a function of polymer concentration or of the molecular weight of the polymer), this ξ decreases

with increasing polymer concentration (c). Thus, the self-diffusion coefficient of the diffusant decreases when the polymer concentration increases. However, in the viscous gel regime, the correlation length decreases more slowly. Thus, the effect of the polymer concentration on the self-diffusion coefficient tends to be less significant, as illustrated in Figure 3. The viscous gel regime is determined by many factors such as the molecular interactions and the molecular weight of the polymer. In the case of PVA, the degree of hydrolysis is also an important factor. Figure 3 also shows a dependence of the self-diffusion coefficients on the molecular weight or the molecular size. However, this molecular weight effect becomes less significant for dendrimers with higher molecular weights. This trend is more obvious at higher PVA concentrations for PPI(TEO)₃₂ and PPI(TEO)₆₄ dendrimers.

Dashed lines in Figure 3 represent the result of the fit to the model of Petit et al.¹¹

$$D = \frac{D_0}{1 + ac^{2\nu}} \quad (7)$$

where $a = D_0/k\beta^2$, ν is a constant, which is characteristic of the polymer–solvent system, k represents the jump frequency over the energy barriers, which is expected to depend on temperature and size of the diffusant, and c is the polymer concentration. This jump frequency can be written in an Arrhenius form:

$$k = F_p \exp\left(\frac{-\Delta E}{k_B T}\right) \quad (8)$$

where F_p is a frequency prefactor and ΔE is the height of the potential barrier. The model of Petit et al. treats the polymer solution as a transient statistical network, through which the diffusant diffuses in a series of jumps over a potential barrier determined by the correlation length. Thus, when ξ decreases, there is an increase in the energy barrier that the diffusant molecule has to overcome to diffuse in the polymeric network.

The model was used to fit the variation of the self-diffusion coefficient as a function of PVA concentration for all dendrimers (and at different temperatures as well). The values of the parameters D_0 , $k\beta^2$, and ν obtained from the fit with eq 7 are listed in Table 3. It shows that excellent agreement of the D_0 values obtained from fitting to the ones measured by the NMR experiments. The margin of errors for all the parameters is very small, indicating the high quality of the fittings. The D_0 values in the table decrease with the molecular weight. This result agrees well with eq 4, which links the self-diffusion coefficient with the inverse of the cubic root of the molecular weight. When the strength of the interactions between the diffusing molecules and the polymer matrix is strong enough, this trend could be reversed. Moreover, we have observed that the $k\beta^2$ parameter decreases with increasing molecular size of the diffusing dendrimers (see Figure 4). The dashed line serves as visual guide of the decrease in $k\beta^2$ and has no physical meaning. Since β remains constant for a given polymer–solvent system,¹¹ the results obtained confirm that an increase in the molecular size leads to a lower jump frequency.^{4,11,27} Consistent with the results reported by Masaro et al. for PEGs as diffusant,¹³ the $k\beta^2$ parameter decreases with the molecular size of the diffusant. For example, the $k\beta^2$ parameter for PEGs

Table 3. Self-Diffusion Coefficients (D_0), Hydrodynamic Radii (R_h), and Fitting $k\beta^2$ and ν Parameters Obtained for the Dendrimers in Aqueous PVA Systems

sample	D_0 (10^{-11} m ² /s)		$k\beta^2$ ^a (10^{-11})	ν ^a	R_h ^b (nm)	rms ^c error
	exptl	calcd ^a				
PPI(TEO) ₈	16.4 ± 0.2	16.4 ± 0.3	0.79 ± 0.09	0.59 ± 0.03	1.21	0.06
PPI(TEO) ₃₂	9.1 ± 0.1	9.1 ± 0.1	0.16 ± 0.01	0.68 ± 0.02	2.18	0.06
PPI(TEO) ₆₄	7.0 ± 0.3	6.9 ± 0.2	0.10 ± 0.02	0.69 ± 0.04	2.86	0.06

^a Obtained as a fitting parameter from eq 7. ^b Calculated from eq 5. ^c Root-mean-square errors of the nonlinear least-squares fitting to eq 7.

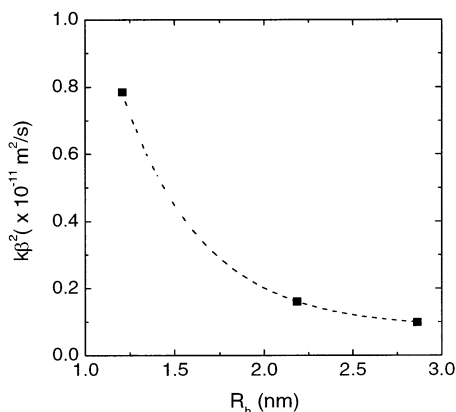


Figure 4. Variation of the $k\beta^2$ parameter as a function of the hydrodynamic radius of the dendrimers at 25 °C. The dashed line is drawn only as visual guide.

with molecular weights of 600, 2000, and 4000 decreased from 1.20×10^{-11} to 0.47×10^{-11} . To compare two diffusants with similar molecular weights, the $k\beta^2$ parameter obtained for PPI(TEO)₈ is 0.79×10^{-11} while that for PEG-2000 is 0.53×10^{-11} , indicating that the jump frequency for the dendrimer is somewhat higher than that of the linear PEG.

The values of the ν parameter in Table 3 are in the same range of the values (0.49–0.76 with an average of ca. 0.58) reported by Masaro et al. for other diffusants in the same polymer–solvent system under the same conditions.^{4,26,27} This ν parameter seems to be characteristic of a given polymer–solvent system and is independent of the diffusing molecule.

The model describes well the variation of the self-diffusion coefficient of the dendrimers in the PVA–water–dendrimer ternary system. Theoretically, the model of Petit et al. should be valid only when c is superior or equal to the critical overlap concentration (c^*), the concentration at which intermolecular entanglements between polymer chains can occur. As shown in Figure 3, the obtained fitting curves with the model of Petit et al. are continuous for the entire concentration range of PVA, including the dilute regime.

Table 3 reports the effective hydrodynamic radius (R_h) obtained for each dendrimer from the Stokes–Einstein equation (eq 5). The hydrodynamic radii for our modified dendrimers are somewhat larger than those obtained by Rietveld et al.⁴⁴ for PPI dendrimers with primary amine end groups. The difference should correspond to the extra length of the added TEO groups on the PPI dendrimers.

The density distribution of dendrimers and linear polymers coils depends on many factors including the quality of the solvent, the temperature, the size of the dendrimer, and the molecular weight of the polymer. To obtain a qualitative evaluation of the density distribution, D_0 and R_h were plotted as a function of the molecular weight. Figure 5A is a logarithmic plot of D_0

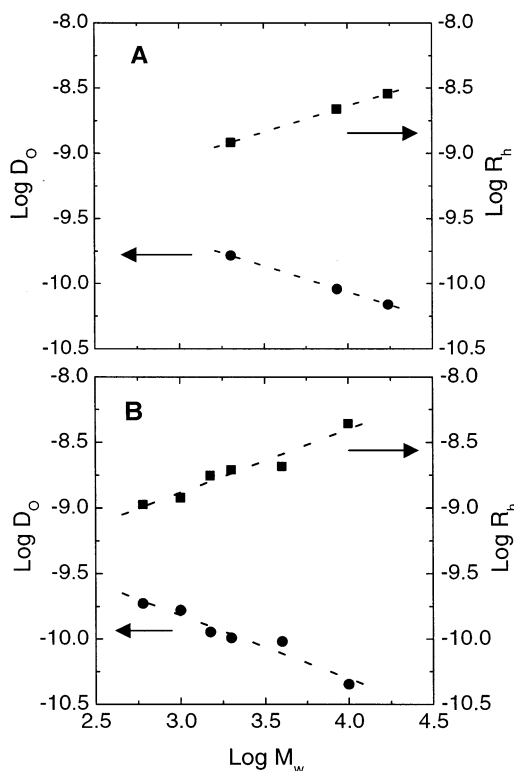


Figure 5. Dependence of D_0 and R_h of dendrimers (A) and PEG (B) on their molecular weights at 25 °C.

and R_h as a function of the molecular weight. The values of the slope obtained for both variations are identical but have opposite signs (slope = 0.40). This result indicates that the density distribution is between a fractal structure (slope = 0.50) and a uniform density distribution (slope = 0.33).⁴⁴ Apparently, the slope of 0.40 differs from that indicated in eq 4 (0.33), but it is important to note that the dendrimers are neither spherical in shape nor uniform in density. It would be interesting to compare the result with that of linear PEGs from the literature.²² The data in Figure 5B show the dependence of D_0 and R_h on the molecular weight for PEGs ($M = 600$ – $10\,000$). The slope obtained for these linear polymers is equal to 0.49, which indicates that the linear diffusants such the PEGs have a fractal density distribution. Understandably, the PEGs as diffusants are less uniform in density than the dendrimers used in this study.

(2) Effect of Temperature. The self-diffusion coefficients of the modified poly(propyleneimine) dendrimers were determined over a temperature range from 5 to 45 °C for eight different PVA concentrations. An example of the results is shown in Figure 6A for the variation of the self-diffusion coefficient of PPI(TEO)₈ dendrimer with PVA concentration (from 0 to 0.26 g/mL). As expected, D increases with increasing temperature, but the effect of temperature becomes less

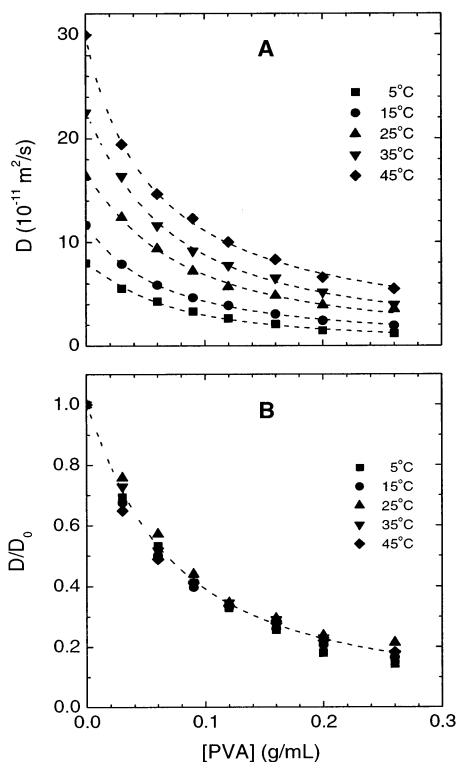


Figure 6. (A) Self-diffusion coefficients and (B) normalized self-diffusion coefficients (D/D_0) of the PPI(TEO)₈ dendrimer as a function of PVA concentration at five different temperatures. Dashed lines are fits to eq 7.

significant with increasing PVA concentration. This decrease is due to the intermolecular entanglements and hydrogen bonding between polymer chains near and above the critical overlap concentration (c^*). In the case of PVA–water system, the c^* is mostly affected by the molecular weight and the degree of hydrolysis, and its value is between 1 and 5% (using the definition $c^* = 1/[\eta]$).^{45–47} It can also be viewed as the concentration of the transition from the dilute regime, where the coils are isolated, to a more concentrated state, where the coils entangle. Above this c^* , a fundamental change in the physical properties of the polymer solutions occurs (e.g., the viscosity behavior).^{48,49} As shown previously,^{45,50} no critical effects have been observed by self-diffusion measurements. The same behavior (i.e., the reduction of the temperature effect on the self-diffusion coefficient at higher PVA concentrations) was observed for the two other dendrimers (PPI(TEO)₃₂ and PPI(TEO)₆₄). Moreover, the effect of the temperature on the self-diffusion coefficient is less significant with increasing molecular weight of the dendrimers (data not shown). This result agrees well with eq 4, which links the self-diffusion coefficient with temperature and the inverse of the cube root of the molecular weight. It is obvious from this equation that D should be less affected by the same temperature variation when the molecular weight is higher.

Another interesting observation is that the dependence of the self-diffusion coefficients of the dendrimer on temperature may be largely contained in the self-diffusion coefficient of the diffusant in the pure solvent (D_0). Figure 6B shows the normalized diffusion coefficients (D/D_0) for the same PPI(TEO)₈ dendrimer as a function of polymer concentration at various temperatures. The data points follow the same trend and are seen to fall more or less on the same line fitted with eq

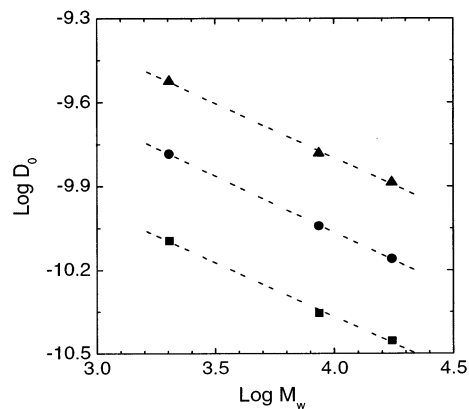


Figure 7. Dependence of D_0 of dendrimers on molecular weight at three different temperatures. Squares, circles, and triangles represent the values obtained at 5, 25, and 45 °C, respectively.

7. Similar results are obtained with the other dendrimers used in this study.

Dashed lines in Figure 6 are the result of the fit with the model of Petit et al. (eq 7). Excellent fitting is obtained for the variation of the self-diffusion coefficient with PVA concentration for all temperatures. The self-diffusion coefficient at zero polymer concentration (D_0) was used to show the effect of the temperature on the density distribution of these three dendrimers (Figure 7). Figure 7 shows the variation of the logarithm of D_0 as a function of the logarithm of molecular weight at three different temperatures (5, 25, and 45 °C). The values of the slope obtained are -0.39 , -0.40 , and -0.39 for 5, 25, and 45 °C, respectively. These results show no effect of the temperature on the density distribution of the dendrimers within this temperature range. From the D_0 values determined with the model of Petit et al., the hydrodynamic radius was calculated with the Stokes–Einstein equation (eq 5) at different temperatures. The results in Figure 8A show a decrease of R_h with increasing temperature for these three dendrimers. However, the decrease is more obvious for dendrimers with higher molecular weight (PPI(TEO)₃₂ and PPI(TEO)₆₄). This may be due to the effect of the quality of the solvent, which decreases with increasing temperature.⁵¹ When the solvent quality decreases, the dendrimers shrink, which leads to a decrease in R_h . This phenomenon affects higher molecular weights first because they are more sensitive to the solvent quality. (This phenomenon is used in the fractionation of polymers.) Stechemesser et al. obtained the same result in their study of the effect of solvent quality on the self-diffusion coefficient of tetrafunctional poly(amidoamine) dendrimers by holographic relaxation spectroscopy.⁵¹ However, this decrease with temperature is small (inferior or equal to 14%). The result in Figure 8A indicates that the properties of these dendrimers may be sensitive to temperature. Figure 8B shows the variation of the ν parameter with temperature. This solvent quality is slightly affected as shown by the small decrease in the value of ν at a higher temperature, but in general, the variation of ν with temperature and with the diffusant is small as shown in Figure 8B, indicating the parameter is characteristic of a given polymer–solvent system.

The variation of the self-diffusion coefficients with the temperature can be used to determine the diffusional activation energy (E_a) with an equation similar to the

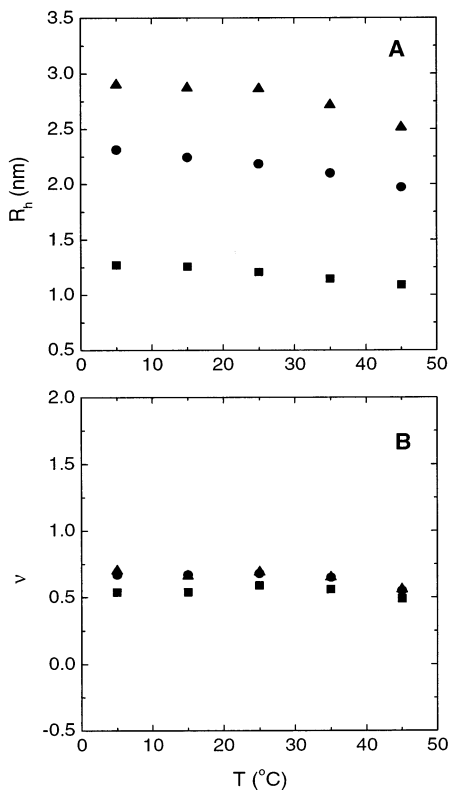


Figure 8. Variation of the hydrodynamic radius (R_h) (A) and the ν parameter in the model of Petit et al. (B) with the temperature for the three dendrimers. Squares, PPI(TEO)₈; circles, PPI(TEO)₃₂; and triangles, PPI(TEO)₆₄.

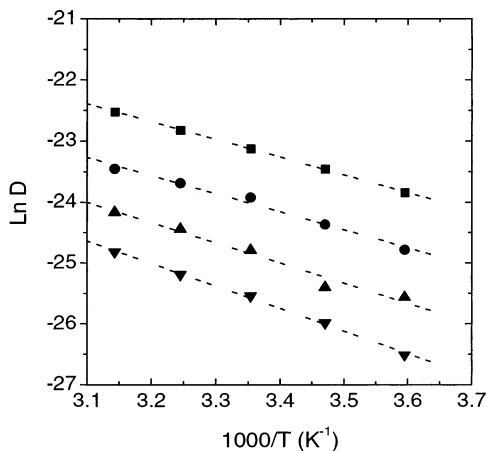


Figure 9. Semilogarithmic plot of the self-diffusion coefficients of the PPI(TEO)₃₂ dendrimer as a function of reciprocal temperature for four PVA concentrations. Squares, 0.00 g/mL; circles, 0.06 g/mL; upward triangles, 0.16 g/mL; and downward triangles, 0.26 g/mL.

Arrhenius equation:

$$D(T) = D_{\infty} \exp(-E_a/RT) \quad (9)$$

where D_{∞} is the self-diffusion coefficient at infinite temperature. Figure 9 shows the temperature dependence of the PPI(TEO)₃₂ dendrimer as a function of the inverse of the temperature for four different PVA concentrations. The Arrhenius equation allows a good fit to the variation of D , observed for all regimes (straight lines in Figure 9), and shows the accuracy of this approach. Figure 9 also shows a continuous increase

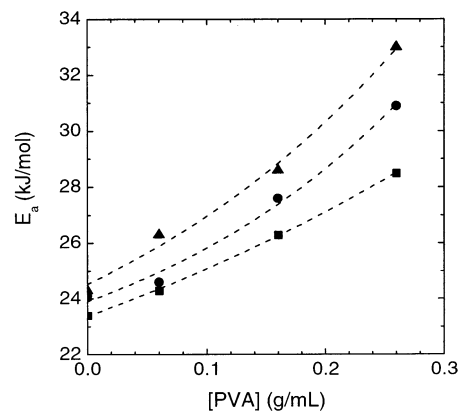


Figure 10. Variation of the diffusional activation energy with the PVA concentration for three dendrimers: Squares, PPI(TEO)₈; circles, PPI(TEO)₃₂; and triangles, PPI(TEO)₆₄. The dashed line is drawn only as visual guide.

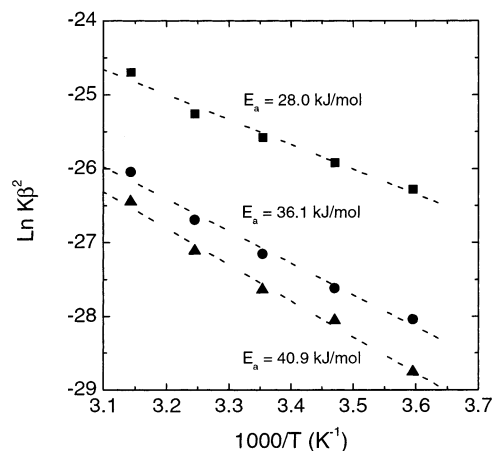


Figure 11. Semilogarithmic plot of the $k\beta^2$ parameter as a function of reciprocal temperature for the three dendrimers. Squares, PPI(TEO)₈; circles, PPI(TEO)₃₂; and triangles, PPI(TEO)₆₄.

of the slope with the polymer concentration, which implies an increase of the diffusional activation energy. This increase is clearly visible in Figure 10, which shows the rapid increase in the diffusional activation energy with the polymer concentration. We can also see an increase of this energy with the molecular weight for each PVA concentration. The dashed line is drawn as visual guides. All these results indicate that the diffusing molecule requires more energy at higher molecular weight and at higher polymer concentration to escape its present surrounding and move into an adjacent environment. As for the determination of diffusional activation energy by the variation of the self-diffusion coefficient with temperature, the same Arrhenius approach was used with the $k\beta^2$ parameter to obtain the apparent activation energy (Figure 11), since we assume that β is a constant within the temperature range studied here. A good linear relationship is obtained for all dendrimers. The apparent activation energies obtained are 28.0, 36.1, and 40.9 kJ/mol for the PPI(TEO)₈, PPI(TEO)₃₂, and PPI(TEO)₆₄ dendrimers, respectively. According to the model of Petit et al.,¹¹ these results confirm that the larger diffusing molecule has a lower jump frequency and thus needs a higher energy to escape its present surrounding to diffuse in the polymeric network. In comparison to the results obtained by Masaro et al. with PEG diffusants,⁴ the energy

barriers of the dendrimers can be related to that obtained for ethylene glycol ($R_h = 0.24$ nm) and two PEG samples with molecular weights of 600 and 2000 ($R_h = 1.25$ and 2.27 nm, respectively), which have E_a values of 30.0, 36.5, and 39.0 kJ/mol, respectively. Although the dendrimers used here generally possess higher molecular weights than the linear PEGs studied, the energy barriers for the dendrimers are much lower in comparison with the linear PEGs. For the one that is comparable in molecular weight, PPI(TEO)₈ has a similar molecular weight as PEG-2000, but its energy barrier is much lower (28 kJ/mol for PPI(TEO)₈ vs 39 kJ/mol for PEG-2000). It is possible that ethylene glycol and PEG can form hydrogen bonds more easily with the polymer matrix and with the aqueous surrounding in comparison to the dendrimers. For each dendrimer, the activation energy value obtained with the model of Petit et al. (Figure 11) is higher than the diffusional activation energy (Figure 10). The difference is not yet well understood. However, it seems that the apparent activation energy obtained from k^2 can be related to the maximum energy that the diffusing molecule has to overcome to diffuse in the polymer matrix at gel polymer concentration.

Conclusion

It is clearly shown that the self-diffusion coefficients of the dendrimers decrease with increasing molecular size of the diffusant, with increasing PVA concentration but with a decreasing temperature. The physical model of Petit et al. has been used successfully to describe the variation of the self-diffusion coefficient with the molecular size of the dendrimer, the polymer concentration, and the temperature. These results show that the larger diffusing molecule needs higher activation energy to escape its present surrounding and to move into an adjacent environment. It is also the case when the polymer concentration increases. The apparent activation energy of diffusion varies in the range 28.0–40.9 kJ/mol from PPI(TEO)₈ to PPI(TEO)₆₄ dendrimers. The study shows that the dendrimers have a density distribution between a fractal structure and a uniform density distribution and that the temperature in the range 5–45 °C has no effect on the density distribution. In comparison to the fractal structure obtained for linear PEGs, dendrimers have a more uniform density distribution. The Stokes–Einstein hard-sphere radii have also been calculated at the zero concentration limit, and we have observed an increase of R_h with the dendrimer generation. However, the results show a slow decrease in R_h with the temperature for these three dendrimers. The study of the motion of different parts of the dendrimers by NMR relaxation time measurements shows that the terminal protons are more mobile than the core protons for all dendrimers. The relaxation time measurements also show a decrease in the mobility for all protons along with increasing dendrimer generation.

Acknowledgment. The financial support from the Natural Sciences and Engineering Research Council (NSERC) of Canada and the National Science Foundation (USA) is gratefully acknowledged.

References and Notes

- (1) Hariharam, D.; Peppas, N. A. *J. Controlled Release* **1993**, *23*, 123–136.
- (2) Clericuzio, M.; Parker, W. O.; Soprani, M.; Andrei, M. *Solid State Ionics* **1995**, *82*, 179–192.
- (3) Gao, P.; Fagerness, P. E. *Pharm. Res.* **1995**, *12*, 955–964.
- (4) Masaro, L.; Zhu, X. X.; Macdonald, P. M. *Macromolecules* **1998**, *31*, 3880–3885.
- (5) Fujita, H. *Adv. Polym. Sci.* **1961**, *3*, 1–47.
- (6) Yasuda, H.; Lamaze, C. E.; Ikenberry, L. D. *Makromol. Chem.* **1968**, *118*, 19–35.
- (7) Vrentas, J. S.; Duda, J. L. *J. Polym. Sci., Polym. Phys. Ed.* **1977**, *15*, 403–416.
- (8) Vrentas, J. S.; Duda, J. L. *J. Polym. Sci., Polym. Phys. Ed.* **1977**, *15*, 417–439.
- (9) Phillies, G. D. J. *Macromolecules* **1986**, *19*, 2367–2376.
- (10) Vrentas, J. S.; Vrentas, C. M. *Macromolecules* **1994**, *27*, 4684–4690.
- (11) Petit, J.-M.; Roux, B.; Zhu, X. X.; Macdonald, P. M. *Macromolecules* **1996**, *29*, 6031–6036.
- (12) Amsden, B. *Macromolecules* **1998**, *31*, 8382–8395.
- (13) Masaro, L.; Zhu, X. X. *Prog. Polym. Sci.* **1999**, *24*, 731–775.
- (14) Nesmelova, I. V.; Skirda, V. D.; Fedotov, V. D. *Biopolymers* **2002**, *63*, 132–140.
- (15) Seland, J. G.; Ottaviani, M.; Hafskjold, Bjørn. *J. Colloid Interface Sci.* **2001**, *239*, 168–177.
- (16) Derrick, T. S.; Larive, C. K. *Appl. Spectrosc.* **1999**, *53*, 1595–1600.
- (17) Penke, B.; Kinsey, S.; Gibbs, S. J.; Moerland, T. S.; Locke, B. R. *J. Magn. Reson.* **1998**, *132*, 240–254.
- (18) Manz, B.; Callaghan, P. T. *Macromolecules* **1997**, *30*, 3309–3316.
- (19) Yokoyama, H.; Kramer, E. J.; Fredrickson, G. H. *Macromolecules* **2000**, *33*, 2249–2257.
- (20) Nydén, M.; Söderman, O. *Macromolecules* **1998**, *31*, 4990–5002.
- (21) Waggoner, R. A.; Blum, F. D.; MacElroy, J. M. D. *Macromolecules* **1993**, *26*, 6841–6848.
- (22) Baille, W. E.; Malveau, C.; Zhu, X. X.; Marchessault, R. H. *Biomacromolecules* **2002**, *3*, 214–218.
- (23) Malveau, C.; Beaume, F.; Germain, Y.; Canet, D. *J. Polym. Sci., Part B: Polym. Phys.* **2001**, *39*, 2781–2792.
- (24) Rollet, A.-L.; Simonin, J.-P.; Turq, P.; Gebel, G.; Kahn, R.; Vandais, A.; Noël, J.-P.; Malveau, C.; Canet, D. *J. Phys. Chem. B* **2001**, *105*, 4503–4509.
- (25) Petit, J.-M.; Zhu, X. X.; Macdonald, P. M. *Macromolecules* **1996**, *29*, 70–76.
- (26) Masaro, L.; Ousalem, M.; Baille, W. E.; Lessard, D.; Zhu, X. X. *Macromolecules* **1999**, *32*, 4375–4382.
- (27) Masaro, L.; Zhu, X. X.; Macdonald, P. M. *J. Polym. Sci., Part B: Polym. Phys.* **1999**, *37*, 2396–2403.
- (28) Masaro, L.; Zhu, X. X. *Macromolecules* **1999**, *32*, 5383–5390.
- (29) Yonetake, K.; Masuko, T.; Morishita, T.; Suzuki, K.; Ueda, M.; Nagahata, R. *Macromolecules* **1999**, *32*, 6578–6586.
- (30) Uppuluri, S.; Keinath, S. E.; Tomalia, D. A.; Dvornic, P. R. *Macromolecules* **1998**, *31*, 4498–4510.
- (31) Scherrenberg, R.; Coussens, B.; van Vliet, P.; Edouard, G.; Brackman, J.; de Brabander, E. *Macromolecules* **1998**, *31*, 456–461.
- (32) Roover, J.; Zhou, L.-L.; Toporowski, P. M.; van der Zwan, M.; Iatrou, H.; Hadjichristidis, N. *Macromolecules* **1993**, *26*, 4324–4331.
- (33) Pan, Y.; Ford, W. T. *Macromolecules* **1999**, *32*, 5468–5470.
- (34) Chai, M.; Niu, Y.; Youngs, W. J.; Rinaldi, P. L. *J. Am. Chem. Soc.* **2001**, *123*, 4670–4678.
- (35) Pan, Y.; Ford, W. T. *Macromolecules* **2000**, *33*, 3731–3738.
- (36) Kreider, J. L.; Ford, W. T. *J. Polym. Sci., Part A: Polym. Chem.* **2001**, *39*, 821–832.
- (37) Tanner, J. E. *J. Chem. Phys.* **1970**, *52*, 2523–2526.
- (38) Callaghan, P. T.; Trotter, C. M.; Jolley, K. W. *J. Magn. Reson.* **1980**, *37*, 247–259.
- (39) Stilbs, P. *Prog. Nucl. Magn. Reson. Spectrosc.* **1987**, *19*, 1–45.
- (40) Price, W. S. *Concepts Magn. Reson.* **1997**, *9*, 299–336.
- (41) Amman, C.; Meier, P.; Merbach, A. E. *J. Magn. Reson.* **1982**, *46*, 319–322.
- (42) Waldeck, A. R.; Kuchel, P. W.; Lennon, A. J.; Chapman, B. E. *Prog. Nucl. Magn. Reson. Spectrosc.* **1997**, *30*, 39–68.
- (43) De Gennes, P. G. *Scaling Concepts in Polymer Physics*; Cornell University Press: Ithaca, NY, 1979.

- (44) Rietveld, I. B.; Bedeaux, D. *Macromolecules* **2000**, *33*, 7912–7917.
- (45) Cosgrove, T.; Griffiths, P. C. *Polymer* **1994**, *35*, 509–513.
- (46) Fang, L.; Brown, W. *Macromolecules* **1990**, *23*, 3284–3290.
- (47) Te Nijenhuis, K. *Adv. Polym. Sci.* **1997**, *130*, 36–52.
- (48) Ferry, J. D. *Viscoelastic Properties of Polymers*; Wiley: New York, 1980.
- (49) Flory, P. J. *Principles of Polymer Chemistry*, Cornell University Press: Ithaca, NY, 1953.
- (50) Skirda, V. D.; Sundukov, V. I.; Maklakov, A. I.; Zgadzai, O. E.; Gaturov, R. R.; Vasiljiev, G. I. *Polymer* **1988**, *29*, 1294–1300.
- (51) Stechemesser, S.; Eimer, W. *Macromolecules* **1997**, *30*, 2204–2206.

MA025636K